Olmesartan inhibits cardiac hypertrophy in mice overexpressing renin independently of blood pressure: its beneficial effects on ACE2/Ang(1-7)/Mas axis and NADPH oxidase expression

(オルメサルタンはレニン過剰発現マウスにおいて血圧非依存的に心肥大を抑制する：ACE2/Ang(1-7)/Mas系とNADPHオキシダーゼ発現への有効性に関する検討)

申請者

弘前大学大学院医学研究科

循環病態科学領域循環病態内科学教育研究分野

氏名　　丹野　倫宏

指導教授　若林　孝一

Abstract

Enhanced renin angiotensin activity causes hypertension and cardiac hypertrophy. The angiotensin (Ang) converting enzyme (ACE)2/Ang(1-7)/Mas axis pathway functions against Ang II type 1 receptor (AT1R) signaling. We investigated whether olmesartan (Olm), an AT1R blocker, inhibits cardiac hypertrophy independently of blood pressure, and evaluated potential mechanisms. The 3-4 month-old male mice overexpressing renin in the liver (Ren-Tg) were given orally Olm (5 mg/kg/day) and hydralazine (Hyd)(3.5 mg/kg/day) for 2 months. Systolic blood pressure (SBP) was higher in the Ren-Tg mice than in wild-type littermates. Olm and Hyd treatments lowered SBP to the same degree. However, cardiac hypertrophy, evaluated by echocardiography, heart weight, cross-sectional area of cardiomyocytes, and gene expression, was inhibited by only Olm treatment, but not by Hyd. Olm treatment reversed decreased gene expressions of ACE2 and Mas receptor of Ren-Tg mice and inhibited enhanced NADPH oxidase (Nox)4 expression and reactive oxygen species, whereas Hyd treatment had no influence to them. These findings indicate that Olm treatment inhibits cardiac hypertrophy independently of blood pressure, not only through its original AT1R blockade but partly through enhancement of ACE2/Ang(1-7)/Mas axis and suppression of Nox4 expression.

Keywords: ACE2, Cardiac hypertrophy, NADPH oxidase, Olmesartan, Renin angiotensin

system

Introduction

Enhanced activity of renin angiotensin system (RAS) causes hypertension and consequently leads to organ damages such as cardiac hypertrophy (1-4). Indeed, previous animal study using mice with a genetically clamped renin transgene in the liver (Ren-Tg mice) demonstrated that an increase in angiotensin (Ang) II causes high blood pressure, thereby resulting in cardiac hypertrophy and renal damage (5, 6). However, it remains to be elucidated whether either high blood pressure or enhanced Ang II activity largely contributes to RAS-induced cardiac hypertrophy.

Angiotensin converting enzyme (ACE)-related carboxypeptidase, ACE2, is an enzyme similar to ACE, and hydrolyzes Ang I to Ang(1-9) and Ang II to Ang(1-7) (7, 8). Ang(1-7) counterregulates Ang II actions via activation of the Mas G protein-coupled receptor (9, 10), and attenuates reactive oxygen species (ROS) partly through decrease in NADPH oxidase (Nox) expression (11-13), which plays a key role in the hypertension-induced ROS generation (14, 15). Thus, ACE2/Ang(1-7)/Mas axis pathway plays a protective role in the cardiovascular system against RAS.

Olmesartan (Olm) is an Ang II type 1 receptor (AT1R) antagonist that can inhibit Ang II-induced cardiac remodeling and heart failure by lowering blood pressure and AT1R blockade (16, 17). Olm administration has also been shown to increase ACE2 expression of the heart in the stroke-prone spontaneously hypertensive rats (18), and in the

experimental rat models of post-myocardial infarction and cardiac-myosin induced dilated cardiomyopathy (19, 20). In the present study, we investigated factors contributing to RAS-induced cardiac hypertrophy and evaluated the inhibitory effects of Olm in comparison with hydralazine (Hyd), a direct vasodilator, using the Ren-Tg mice, highlighting the roles of ACE2/Ang(1-7)/Mas receptor pathway and Nox expression.

Methods

Animals and reagents

The Ren-Tg mice (originally RenTgMK mice) were kindly provided by Drs. Oliver Smithies and Nobuyo Maeda (The University of North Carolina at Chapel Hill, Chapel Hill, NC, USA). Briefly, a modified mouse renin transgene driven by a liver-specific albumin promoter/enhancer was inserted into the genome as a single copy at the liver-specific *ApoA1/ApoC3* locus. The resulting transgene expresses renin ectopically at a constant high level in the liver and leads to elevated plasma levels of active renin and Ang II (5, 6). The 3-4 month-old male heterozygous (one copy of the renin transgene) Ren-Tg mice, backcrossed to C57BL6/N mice more than 6 generations, were used in the present study. The Ren-Tg mice were administered olmesartan medoxomil (5 mg/kg/day; Olm), hydralazine hydrochloride (3.5 mg/kg/day; Hyd), or vehicle (Ren) for 2 months. Drugs were dissolved in their drinking water and given orally. Body weight and the amount of

water consumed by each mouse were measured, and the dose of antihypertensive drugs dissolved in the drinking water to achieve a similar decrease in blood pressure was determined by the preliminary experiments. Wild-type (WT) littermates given vehicle were used as a control. The four groups, i.e., WT, Ren, Olm, and Hyd groups, were compared in the following experiments. Olm was kindly provided by Daiichi-Sankyo Co., Ltd (Tokyo, Japan). Hyd was purchased from Sigma-Aldrich (St. Louis, MO, USA). All procedures were performed in accordance with the Guide for the Care and Use of Laboratory Animals of the National Institutes of Health (NIH) and were approved by the Institutional Animal Care and Use Committee of Hirosaki University Graduate School of Medicine.

Blood pressure measurement

Mice were kept in a warmed chamber at 37° C for approximately 10 minutes, and then systolic blood pressure (SBP) and pulse rate (PR) were measured in conscious mice by the tail-cuff method (BP-98A; Softron, Tokyo, Japan). After the highest and lowest readings were discarded, at least 10 readings were averaged each day for continuous 3 days.

Echocardiography

Ultrasound studies were performed using an echocardiography system (HD11 XE with L15-7io Broadband Compact Linear Array; Phillips, Eindhoven, The Netherlands) in conscious mice. Briefly, mice were laid on a heating pat maintained at 37° C in the supine

position and the anterior chest area was shaved. Warmed gel was applied to the anterior chest of examined mice and M-mode tracing was recorded from short-axis view at the papillary muscle level. Interventricular septum in diastole (IVSd), left ventricular posterior wall thickness in diastole (LVPWd), left ventricular end-diastolic dimension (LVDd) and end-systolic dimension (LVDs) were measured and the data from at least 3 cardiac cycles were averaged. Fractional shortening (FS) was calculated as [(LVDd-LVDs)/LVDd] x 100. Two experienced cardiologists blindly reviewed all the images.

Real-time reverse-transcription polymerase chain reaction (real-time RT-PCR)

After mice were euthanized by cervical dislocation under anesthesia with medetomidine (0.75 mg/kg), midazolam (4 mg/kg), and butorphanol tartrate (5 mg/kg) by intraperitoneal route, the heart was immediately excised and cut transversely at the papillary muscle level. The upper part of left ventricle was used to perform RT-PCR examination and evaluate ROS generation. The lower one was used to evaluate histological examinations. Total RNA was isolated from left ventricle with RNeasy® Fibrous Tissue Mini Kit (QIAGEN, Hilden, Germany) according to the manufacturer's protocol. The RNA was converted into cDNA with PrimeScript™ II 1st Strand cDNA Synthesis Kit (Takara Bio Inc., Shiga, Japan). Real-time RT-PCR was performed using the TaqMan® Gene Expression Assays (Life Technologies, Gaithersburg, MD, USA). The samples were heated to 95° C for 10 min, and 40 cycles of a two-step PCR were performed (95° C for 15 s and 60° C for

60 s). The gene expression of the samples was normalized to their glyceraldehyde-3-phosphate dehydrogenase (GAPDH) contents and then described as a ratio to WT group (control). The primers and the Taqman probe for the target genes, α-myosin heavy chain (α-MHC), β-MHC, brain natriuretic peptide (BNP), transforming growth factor-β1 (TGF-β1), collagen I, ACE2, Mas, Nox2, and Nox4, were purchased from Life Technologies and summarized in the Supplemental Table.

Histological examinations

The lower part of ventricle samples was fixed in 10% formalin, embedded in paraffin, and stained with hematoxylin and eosin (H&E) for measurement of cardiomyocyte hypertrophy and with Masson trichrome for evaluation of cardiac fibrosis. Stained sections were examined using a Keyence all-in-one fluorescence microscope BZ-X710 (Keyence, Osaka, Japan). Three or four different fields were selected to measure the cross-sectional area (CSA) of cardiomyocytes, and 50-70 randomly selected cardiomyocytes were analyzed with image analysis programs, NIH Image J and BZ-X Analyzer (Keyence, Osaka, Japan).

Evaluation of ROS generation in the heart

To evaluate ROS generation in the heart, we measured protein carbonyl levels, an indicator of oxidative stress, using OxyBlot™ protein oxidation detection kit (Chemicon, USA) according to the manufacturer's detailed instructions (21). The protein

bands were detected by Amersham ECL Prime Western Blotting Detection Reagents (GE Healthcare, Buckinghamshire, UK). Levels of oxidatively modified proteins were quantified using NIH Image J.

Statistical analysis

All data are shown as mean±SEM. Statistical analyses were performed with a commercially available software program JMP Pro 11.1.1 (SAS, Cary, NC, USA). Multiple comparisons were performed by ANOVA followed by Tukey's honestly significant difference. A p-value of <0.05 was considered to be significant.

Results

Effects of Olm and Hyd treatments on blood pressure

Blood pressure before treatment was significantly higher in all groups of the Ren-Tg mice than in the WT group (Table 1). After each treatment for 2 months, the Ren group showed still higher blood pressure than the WT group (121±2 versus 104±2 mmHg, n=6, $p<0.05$). Blood pressures in the Olm and Hyd groups after 2 months were similar and significantly lower than that in the Ren group (93±4 and 91±3 versus 121±2 mmHg, n=6, both $p<0.05$). There was no difference in pulse rate among the all groups before and after treatment (Table 1).

Effects of Olm and Hyd treatments on cardiac hypertrophy

Echocardiography showed that IVSd and LVPWd (mm) were significantly thicker in the Ren group than in the WT group (0.95±0.02 versus 0.74±0.05 for IVSd, and 0.91±0.07 versus 0.71±0.04 for LVPWd, respectively, n=6, both $p<0.05$) (Table 2). Olm treatment attenuated these thickened IVSd and LVPWd (0.72±0.05 and 0.70±0.01, n=6, $p<0.05$), but Hyd treatment did not (0.94±0.03 and 0.92±0.03, n=6). LVDd, LVDs, and FS were not different among the four groups.

The ratio of heart to body weight (HW/BW) was measured after treatment for 2 months (Table 2). The BW did not differ among the four groups. The HW was significantly higher in the Ren group than in the WT group ($p<0.05$). Olm treatment attenuated the increased HW, whereas Hyd treatment did not. Consistent with this, the HW/BW (mg/g) was significantly higher in the Ren group than in the WT group (5.1±0.2 versus 4.1±0.1, n=6, $p<0.05$). Olm treatment inhibited the increase in HW/BW (4.6±0.3), whereas Hyd treatment had no influence on it (5.3±0.1) (Table 2). Histological assessment further showed that LV hypertrophy was found in the Ren group (Figure 1A). Olm treatment attenuated LV hypertrophy, whereas Hyd treatment did not. Consistent with this, hypertrophy of cardiomyocytes was observed in the Ren and the Hyd groups, but not in the Olm group (Figure 1B). Quantitative analysis showed that CSA ratio of cardiomyocytes was significantly greater in the Ren group than in the WT group (1.32±0.05 versus 1.00±0.09, n=7, $p<0.05$)(Figure 1C). Olm treatment attenuated the increased CSA to the

similar degree as in the WT group (0.81±0.05, n=6, $p<0.05$ versus Ren group), whereas Hyd treatment had no influence on it (1.31±0.04, n=6) (Figure 1C).

The gene expression of BNP was significantly higher in the Ren than in the WT groups (4.56±1.17, n=7, $p<0.05$ versus WT group)(Figure 1D). Olm treatment significantly decreased the BNP expression (1.75±0.38, n=6, $p<0.05$ versus Ren group), whereas Hyd treatment did not (3.76±0.28, n=6). The ratio of the fetal type MHC, β-MHC, to the adult-type α-MHC, β-MHC/α-MHC, was remarkably increased in the Ren than in the WT groups (8.02±2.04, n=7, $p<0.05$) (Figure 1D). Olm treatment completely blocked the increased ratio observed in the Ren group (1.12±0.19, n=6, $p<0.05$), whereas Hyd treatment did not (9.11±2.00, n=6).

Effects of Olm and Hyd treatments on cardiac fibrosis and vascular wall thickness

There was no significant difference in interstitial fibrosis of the heart among the four groups (Figure 2A). The gene expression of TGF-β1 was significantly higher in the Ren than in the WT groups (1.37±0.11, n=7, $p<0.05$ versus WT group)(Figure 2B). Olm and Hyd treatments inhibit its increase to the similar degree as in the WT group (1.16±0.03 and 0.99±0.06, n=7). Collagen I expression tended to be increased in the Ren group compared with the WT group (1.26±0.07, n=6-7, $p=0.07$ versus WT group). Olm and Hyd treatments completely blocked its increase (0.70±0.09 and 0.76±0.08, n=6-7, both $p<0.05$ versus Ren group)(Figure 2B).

Effects of Olm and Hyd treatments on gene expression of ACE2/Mas axis

The gene expression of ACE2 and Mas in the Ren group was significantly decreased compared with that in the WT group (0.57±0.02 for ACE2 and 0.51±0.11 for Mas, respectively, n=6-7, both $p<0.05$ versus WT group). The decrease in their gene expression observed in the Ren group was completely recovered by Olm treatment to the same degree as in the WT group (0.96±0.08 for ACE2 and 1.04±0.13 for Mas, respectively, n=6, both $p<0.05$ versus Ren group), but Hyd treatment did not improve their gene expression (0.72±0.04 for ACE2 and 0.51±0.06 for Mas, n=6)(Figure 3).

Effects of Olm and Hyd treatments on gene expression of NADPH oxidases and ROS generation

Activation of Nox plays a major role in Ang II-mediated ROS generation (22). The gene expression of Nox2 was not different among the four groups (Figure 4A). In contrast, the gene expression of Nox4 was significantly higher in the Ren than in the WT groups (2.40±0.25, n=7, $p<0.05$ versus WT group). Olm treatment significantly decreased the Nox4 expression (0.71±0.06, n=7, $p<0.05$ versus Ren group), whereas Hyd treatment did not (1.71±0.24, n=6) (Figure 4B).

Protein carbonyl level in the heart was increased in the Ren group compared with the WT group (2.39±0.31 versus 1.00±0.17, $p<0.05$, n=3) (Figure 4C). Olm treatment inhibited them (1.46±0.05, $p<0.05$ versus Ren group, n=3), but not Hyd treatment (2.12±0.03, n=3).

Discussion

Major findings

In the present study, we showed that treatment with Olm or Hyd for 2 months similarly lowered an elevated SBP in the Ren-Tg mice, but only Olm treatment inhibited cardiac hypertrophy in the Ren-Tg mice. Furthermore, Olm treatment reversed decreased gene expressions of ACE2 and Mas receptor observed in the Ren-Tg mice and inhibited an enhanced Nox4 gene expression and ROS generation, whereas Hyd treatment had no influence on them. These findings indicate that Olm treatment inhibits cardiac hypertrophy independently of blood pressure, not only through its original AT1R blockade but partly through enhancement of ACE2/Ang(1-7)/Mas axis pathway and suppression of Nox4 expression in the heart.

Effects of Olm on cardiac hypertrophy

The Ren-Tg mice have a genetically clamped renin transgene, which was first reported by Caron et al. as a lifelong genetic minipump (5, 6, 23), because renin production is regulated by liver-specific albumin promoter/enhancer and therefore it is insensitive to homeostatic feedback. Plasma renin concentration in this mouse model is reported to be 8 times higher than in WT controls (23). As expected, the Ren-TG mice have high blood pressure and concentric cardiac hypertrophy caused by an increase in

Ang II through the AT1R signaling (6, 23). Consistent with this, the present study also showed high blood pressure and cardiac hypertrophy in the Ren-Tg mice, as demonstrated by echocardiography and histological assessments. Importantly, their cardiomyocytes are exposed to two hypertrophic stimuli: an increased blood pressure and an increased level of plasma Ang II. To understand the role of each stimulus in cardiac hypertrophy, we administered two antihypertensives to the Ren-Tg mice: Olm (a depressor by AT1R blockade) and Hyd (a direct vasodilator). The results clearly showed that only Olm treatment inhibited cardiac hypertrophy, although both antihypertensives similarly lowered an elevated blood pressure observed in the Ren-Tg mice. Furthermore, our results are supported by the previous report showing that treatment with lisinopril, an ACE inhibitor, or Hyd, both lowered SBP in the Tsukuba hypertensive transgenic mice carrying human renin and angiotensinogen genes (24), but only lisinopril inhibited cardiac hypertrophy. These findings indicate that enhanced AT1R signaling by an increased RAS activity, not high blood pressure, is considerably important to the progression of cardiac hypertrophy.

To investigate the molecular phenotype of the cardiac hypertrophy, expression analyses of the genes involved in the progression of cardiac hypertrophy were performed. Increased gene expression of BNP and high ratio of β-MHC/α-MHC found in the Ren-Tg mice were decreased by Olm treatment but not by Hyd treatment. These findings also support inhibitory effect of Olm treatment on cardiac hypertrophy.

Effects of Olm on cardiac fibrosis

Cardiac hypertrophy and fibrosis are closely linked each other (25). TGF-β1 and collagen I are an important mediator for cardiac fibrosis induced by Ang II (25-28). In the present study, increased expression of these genes was found in the Ren-Tg mice, whereas both Olm and Hyd treatments inhibited their increases observed in the Ren-Tg mice. Although interstitial fibrosis of the heart was not observed or a bit in the 6-month-old Ren-Tg mice, and even in those at the age of 8 months (data not shown), our gene expression analysis indicates possible involvement of Olm and Hyd treatments in initial fibrosis process such as perivascular fibrosis. Further studies are required to clarify the process of cardiac and perivascular fibrosis and effects of these agents on it in this mouse model.

Potential mechanisms involved in the inhibitory effect of Olm on cardiac hypertrophy

Ablation of ACE2 in mice causes severe cardiac dysfunction and coronary artery remodeling with enhanced perivascular fibrosis, indicating its protective role in cardiac function (29, 30). Patel et al. also showed that Ang II infusion in the WT mice suppressed ACE2 protein levels and its activity of the heart (31). Furthermore, Ishiyama et al. showed that Olm treatment increases ACE2 gene expression of the heart in post-myocardial infarction rat model (19). In agreement with these findings, the present study showed that the gene expressions of ACE2 and Mas receptor were decreased in the

Ren-Tg mice, and Olm treatment improved their gene expressions, but not Hyd treatment. Thus, Olm treatment may have cardio-protective effects not only through AT1R blockade, but partly through activation of ACE2/Ang(1-7)/Mas axis pathway.

It is of considerable importance to elucidate the mechanism by which AT1R blockade causes the elevation of ACE2 gene expression. Patel et al. showed that activated Ang II-AT1R signaling generates ROS, which in turn results in p38 mitogen-activated protein kinase (MAPK) signaling activation (31). ACE2 mRNA expression has been shown to be suppressed by ROS-induced p38 MAPK signaling activation and Ang II-AT1R signaling blockade by ARB reversed the suppression of ACE2 mRNA expression (32, 33). These reports indicate that Ang II-AT1R signaling pathway regulates ACE2 gene expression, in part through ROS-mediated p38 MAPK signaling. Since ROS is a key regulator for ACE2 gene expression, we measured ROS generation in the heart and found the inhibitory effect of Olm treatment on the ROS generation. This is also supported by the fact that increased gene expression of Nox4 in the Ren-Tg mice was suppressed by Olm treatment in the present study. Consistent with this, Sukumaran reported that Olm treatment upregulated ACE2 gene expression by suppressing ROS generation and p38 MAPK signaling, which in turn resulting in improved cardiac function in dilated cardiomyopathy rat model (20). These findings further indicate that the beneficial effects of Olm on ACE2 gene expression are partly mediated by inhibition of Ang II-AT1R-associated ROS generation.

Conclusions

The present study provides evidence that Olm treatment inhibits cardiac hypertrophy independently of blood pressure, not only through its original AT1R blockade but partly through inhibition of ROS generation and enhancement of ACE2/Ang(1-7)/Mas axis pathway. The beneficial effects of Olm treatment on RAS-induced cardiac hypertrophy, therefore, have important clinical implications for cardiovascular protection in humans.

Acknowledgements

We gratefully thank Misato Kawai, Nahomi Miyamoto and Ritsuko Kasai for their excellent technical supports.

References

1. Mehta PK, Griendling KK. Angiotensin II cell signaling: physiological and pathological effects in the cardiovascular system. *Am J Physiol Cell Physiol.* 2006;292:C82-C97.

2. Kai T, Sugimura K, Shimada S, et al. Renin-angiotensin system stimulates cardiac and renal disorders in Tsukuba hypertensive mice. *Clin Exp Pharmacol Physiol.* 1999;26:206-211.

3. Mazzolai L, Pedrazzini T, Nicoud F, et al. Increased cardiac angiotensin II levels induce right and left ventricular hypertrophy in normotensive mice. *Hypertension.* 2000;35:985-991.

4. Wang HD, Xu S, Johns DG, et al. Role of NADPH oxidase in the vascular hypertrophic and oxidative stress response to angiotensin II in mice. *Circ Res.* 2001;88:947-953.

5. Caron KM, James LR, Kim HS, et al. A genetically clamped renin transgene for the induction of hypertension. *Proc Natl Acad Sci U S A.* 2002;99:8248-8252.

6. Caron KM. Cardiac hypertrophy and sudden death in mice with a genetically clamped renin transgene. *Proc Natl Acad Sci U S A*. 2004;101:3106-3111.

7. Tipnis SR, Hooper NM, Hyde R, et al. A Human Homolog of Angiotensin-converting Enzyme: Cloning and functional expression as a captopril-insensitive carboxypeptidase. *J Biol Chem*. 2000;275:33238-33243.

8. Donoghue M, Hsieh F, Baronas E, et al. A novel angiotensin-converting enzyme-related carboxypeptidase (ACE2) converts angiotensin I to angiotensin 1-9. *Circ Res*. 2000;87:e1-e9.

9. Santos RA, Simoes e Silva AC, Maric C, et al. Angiotensin-(1-7) is an endogenous ligand for the G protein-coupled receptor Mas. *Proc Natl Acad Sci U S A*. 2003;100:8258-8263.

10. Santos RA, Ferreira AJ, Verano-Braga T, et al. Angiotensin-converting enzyme 2, angiotensin-(1-7) and Mas: new players of the renin-angiotensin system. *J Endocrinol*. 2013;216:R1-R17.

11. Gwathmey TM, Pendergrass KD, Reid SD, et al. Angiotensin-(1-7)-angiotensin-converting enzyme 2 attenuates reactive oxygen species formation to angiotensin II within the cell nucleus. *Hypertension*. 2010;55:166-171.

12. Zheng JL, Li GZ, Chen SZ, et al. Angiotensin Converting Enzyme 2/Ang-(1-7)/Mas Axis Protects Brain from Ischemic Injury with a Tendency of Age-dependence. *CNS Neurosci Ther*. 2014;20:452-459.

13. Sampaio WO, Henrique de Castro C, Santos RAS, et al. Angiotensin-(1-7) counterregulates angiotensin II signaling in human endothelial cells. *Hypertension*. 2007;50:1093-1098.

14. Rabelo LA, Alenina N, Bader M. ACE2-angiotensin-(1-7)-Mas axis and oxidative stress in cardiovascular disease. *Hypertens Res.* 2011;34:154-160.

15. Touyz RM. Reactive oxygen species, vascular oxidative stress, and redox signaling in hypertension: what is the clinical significance? *Hypertension*. 2004;44:248-252.

16. Nishio M, Sakata Y, Mano T, et al. Therapeutic effects of angiotensin II type 1 receptor blocker at an advanced stage of hypertensive diastolic heart failure. *J Hypertens*. 2007;25:455-461.

17. Yoshida K, Kohzuki M. Clinical and experimental aspects of olmesartan medoxomil, a new angiotensin II receptor antagonist. *Cardiovasc Drug Rev*. 2004;22:285-308.

18. Agata J, Ura N, Yoshida H, et al. Olmesartan is an angiotensin II receptor blocker with an inhibitory effect on angiotensin-converting enzyme. *Hypertens Res*. 2006;29:865-874.

19. Ishiyama Y, Gallagher PE, Averill DB, et al. Upregulation of angiotensin-converting enzyme 2 after myocardial infarction by blockade of angiotensin II receptors. *Hypertension*. 2004;43:970-976.

20. Sukumaran V, Veeraveedu PT, Lakshmanan AP, et al. Olmesartan medoxomil treatment potently improves cardiac myosin-induced dilated cardiomyopathy via the modulation of ACE-2 and ANG 1-7 mas receptor. *Free Radic Res*. 2012;46:850-860.

21. Saito S, Fujiwara T, Matsunaga T, et al. Increased Adiponectin synthesis in the visceral adipose tissue in men with coronary artery disease treated with pravastatin: A role of the attenuation of oxidative stress. *Atherosclerosis*. 2008;199:378-383.

22. Rajagopalan S, Kurz S, Münzel T, et al. Angiotensin II-mediated hypertension in the rat increases vascular superoxide production via membrane NADH/NADPH oxidase activation. Contribution to alterations of vasomotor tone. *J Clin Invest*. 1996;97:1916-1923.

23. Caron KM, James LR, Lee G, et al. Lifelong genetic minipumps. *Physiol Genomics*. 2005;20:203-209.

24. Kai T, Kino H, Ishikawa K. Role of the renin-angiotensin system in cardiac hypertrophy and renal glomerular sclerosis in transgenic hypertensive mice carrying both human renin and angiotensinogen genes. *Hypertens Res*. 1998;21:39-46.

25. Nicoletti A, Michel JB. Cardiac fibrosis and inflammation: interaction with hemodynamic and hormonal factors. *Cardiovasc Res*. 1999;41:532-543.

26. Williams B. Angiotensin II and the pathophysiology of cardiovascular remodeling. *Am J Cardiol*. 2001;87:10C-17C.

27. Schultz JEJ, Witt SA, Glascock BJ, et al. TGF-β1 mediates the hypertrophic cardiomyocyte growth induced by angiotensin II. *J Clin Invest*. 2002;109:787-796.

28. Ruiz-Ortega M, Rodríguez-Vita J, Sanchez-Lopez E, et al. TGF-β signaling in vascular fibrosis. *Cardiovasc Res*. 2007;74:196-206.

29. Moritani T, Iwai M, Kanno H, et al. ACE2 deficiency induced perivascular fibrosis and cardiac hypertrophy during postnatal development in mice. J Am Soc Hypertens. 2013;7:259-266.

30. Crackower MA, Sarao R, Oudit GY, et al. Angiotensin-converting enzyme 2 is an essential regulator of heart function. *Nature*. 2002;417:822-828.

31. Patel VB, Clarke N, Wang Z, et al. Angiotensin II induced proteolytic cleavage of myocardial ACE2 is mediated by TACE/ADAM-17: A positive feedback mechanism in the

RAS. *J Mol Cell Cardiol*. 2014;66:167-176.

32. Koka V, Huang XR, Chung ACK, et al. Angiotensin II up-regulates angiotensin I-converting enzyme (ACE), but down-regulates ACE2 via the AT1-ERK/p38 MAP kinase pathway. *Am J Pathol*. 2008;172:1174-1183.

33. Gallagher PE, Ferrario CM, Tallant EA. Regulation of ACE2 in cardiac myocytes and fibroblasts. *Am J Physiol: Heart Circ Physiol*. 2008;295:H2373-H2379.

Figure legends

Figure 1. Assessment of cardiac hypertrophy. **A**, Representative images (×40) of the hearts stained with hematoxylin and eosin in the WT, Ren, Olm, and Hyd groups. **B**, High power field (×400). **C**, Comparisons of the ratio of cross sectional area of cardiomyocytes among the four groups. Data were shown as a ratio to WT group (control). n=6-7. **D**, Comparisons of the gene expression of cardiac hypertrophy markers, brain natriuretic peptide (BNP) and the ratio of β- myosin heavy chain (MHC)/α-MHC, in the heart among the four groups. The data were normalized to glyceraldehyde-3-phosphate dehydrogenase (GAPDH) and described as a ratio to the WT group (control). n=6-7.

Figure 2. Assessment of cardiac fibrosis. **A**, Representative images (×100) of the hearts stained with Masson trichrome in the WT, Ren, Olm, and Hyd groups. **B**, Comparisons of the gene expression of cardiac fibrosis markers, transforming growth factor β1 (TGF □1) and collagen I, in the heart among the four groups. The data were normalized to GAPDH and described as a ratio to the WT group (control). n=6-7.

Figure 3. Comparisons of the gene expression of angiotensin converting enzyme 2 (ACE2) (**A**) and Mas receptor (Mas) (**B**) in the heart among the WT, Ren, Olm, and Hyd groups. The data were normalized to GAPDH and described as a ratio to the WT group (control). n=6-7.

Figure 4. Comparisons of the gene expression of NADPH oxidases (Nox) (**A**, Nox2, and **B**, Nox4) and protein carbonyl levels (**C**) in the heart among the WT, Ren, Olm, and Hyd groups. The data of the gene expressions were normalized to GAPDH and described as a ratio to the WT group (control). n=6-7. The data of the protein carbonyl levels were also described as a ratio to the WT group. n=3.

Figure 1

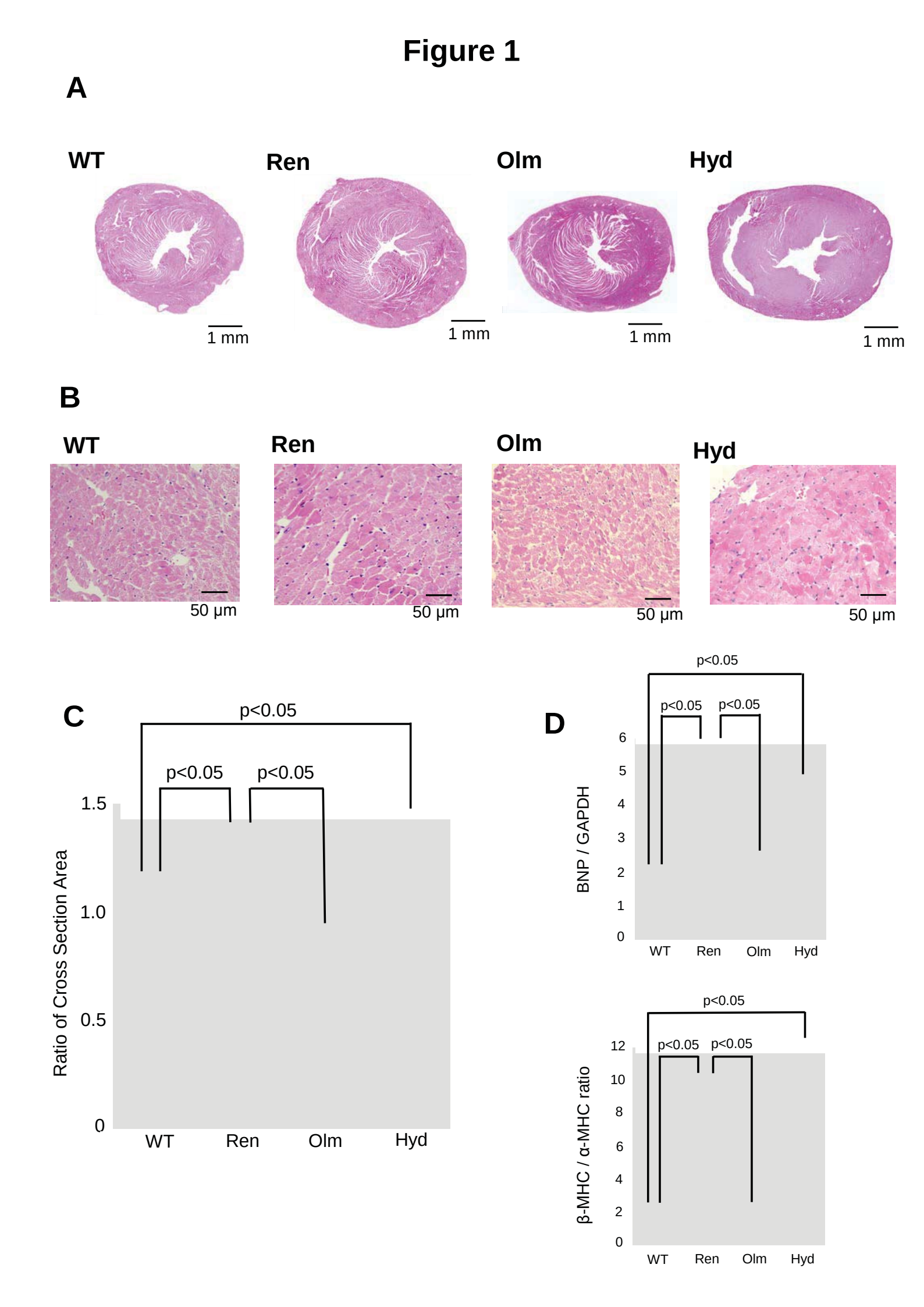
A
WT
Ren
Olm
Hyd
1 mm
1 mm
1 mm
1 mm
B
WT
Ren
Olm
Hyd
50 μm
50 μm
50 μm
50 μm
C
p<0.05
p<0.05
p<0.05
Ratio of Cross Section Area
1.5
1.0
0.5
0
WT
Ren
Olm
Hyd
D
p<0.05
p<0.05
p<0.05
BNP / GAPDH
6
5
4
3
2
1
0
WT
Ren
Olm
Hyd
p<0.05
p<0.05
p<0.05
β-MHC / α-MHC ratio
12
10
8
6
4
2
0
WT
Ren
Olm
Hyd

Figure 2

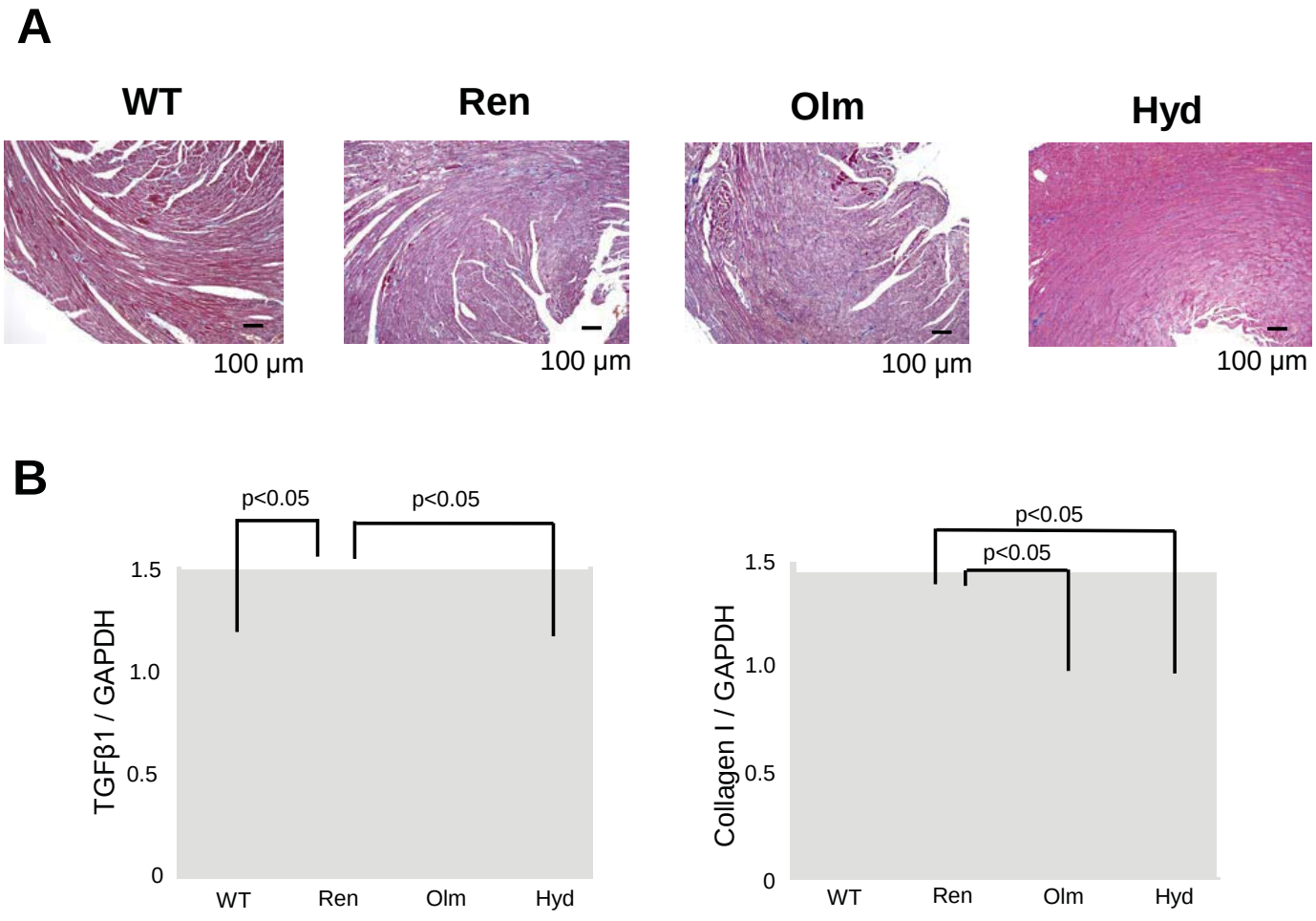
A
WT
Ren
Olm
Hyd
100 µm
100 µm
100 µm
100 µm
B
p<0.05
p<0.05
TGFβ1 / GAPDH
1.5
1.0
0.5
0
WT
Ren
Olm
Hyd
p<0.05
p<0.05
Collagen I / GAPDH
1.5
1.0
0.5
0
WT
Ren
Olm
Hyd

Figure 3

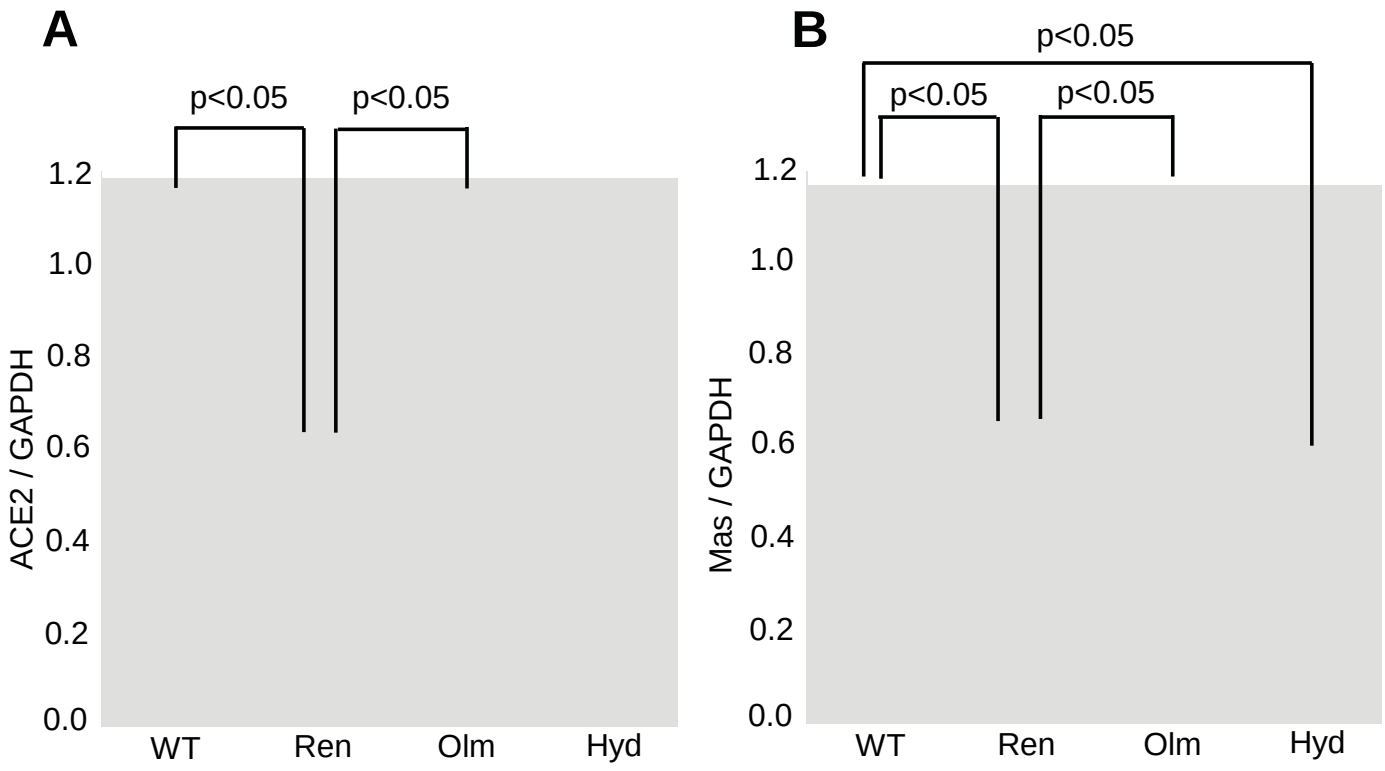
A
p<0.05
p<0.05
1.2
1.0
0.8
0.6
0.4
0.2
0.0
ACE2 / GAPDH
WT
Ren
Olm
Hyd
B
p<0.05
p<0.05
p<0.05
1.2
1.0
0.8
0.6
0.4
0.2
0.0
Mas / GAPDH
WT
Ren
Olm
Hyd

Figure 4

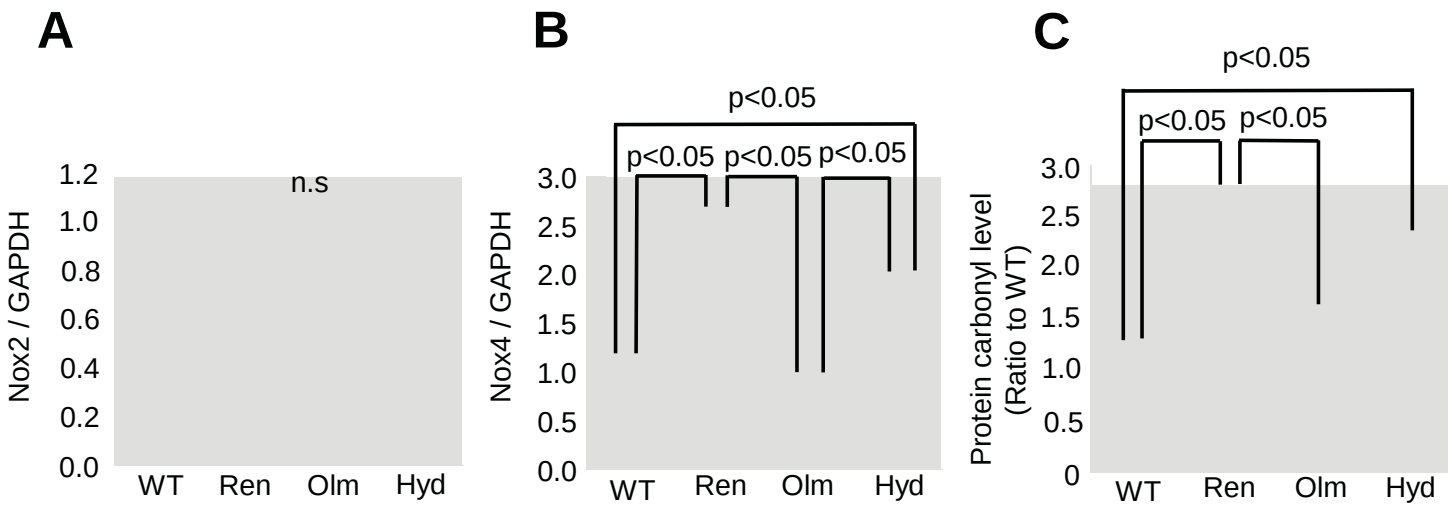
A
Nox2 / GAPDH
1.2
1.0
0.8
0.6
0.4
0.2
0.0
n.s
WT
Ren
Olm
Hyd
B
Nox4 / GAPDH
3.0
2.5
2.0
1.5
1.0
0.5
0.0
p<0.05
p<0.05
p<0.05
p<0.05
WT
Ren
Olm
Hyd
C
Protein carbonyl level
(Ratio to WT)
3.0
2.5
2.0
1.5
1.0
0.5
0
p<0.05
p<0.05
p<0.05
WT
Ren
Olm
Hyd

Table 1. Blood pressure and pulse rate in mice before and after treatment

	WT (n=6)	Ren (n=6)	Olm (n=6)	Hyd (n=6)
Before treatment				
SBP (mmHg)	100±2	116±4[a]	113±3[a]	126±2[a]
PR (bpm)	706±8	695±12	672±11	693±16
After treatment				
SBP (mmHg)	104±2	121±2[b]	93±4	91±3
PR (bpm)	721±9	730±5	707±5	712±11

Data are shown as mean±SEM. SBP indicates systolic blood pressure, PR; pulse rate, WT; wild-type littermates (WT group), Ren; Ren-Tg mice treated with vehicle (Ren group), Olm; Ren-Tg mice treated with olmesartan (Olm group), Hyd; Ren-Tg mice treated with hydralazine (Hyd group).

[a]$p<0.05$ versus WT group, [b]$p<0.05$ versus WT, Olm, and Hyd groups.

Table 2. Echocardiographic parameters and body/heart weight in mice after each treatment for 2 months

	WT (n=6)	Ren (n=6)	Olm (n=6)	Hyd (n=6)
Echocardiography				
IVSd (mm)	0.74±0.05	0.95±0.02[a]	0.72±0.05[b]	0.94±0.03[a]
LVPWd (mm)	0.71±0.04	0.91±0.07[a]	0.70±0.01[b]	0.92±0.03[a]
LVDd (mm)	3.47±0.16	3.00±0.17	3.23±0.10	3.00±0.19
LVDs (mm)	2.17±0.16	1.68±0.23	1.99±0.06	1.67±0.14
FS (%)	37.9±2.5	45.2±4.4	38.5±1.5	44.9±1.8
Body/Heart weight				
BW (g)	33.1±1.0	31.0±1.4	32.3±1.2	32.4±1.2
HW (mg)	137.5±5.4	164.3±8.9[a]	148.7±6.4	171.5±4.8[a]
HW/BW (mg/g)	4.1±0.1	5.1±0.2[a]	4.6±0.3	5.3±0.1[a]

Data are shown as mean±SEM. IVSd indicates interventricular septum in diastole, LVPWd; left ventricular posterior wall thickness in diastole, LVDd; left ventricular dimension in diastole, LVDs; left ventricular dimension in systole, FS; fractional shortening, BW; body weight, HW; heart weight,

[a]$p<0.05$ versus WT group, [b]$p<0.05$ versus Ren and Hyd groups.

Supplemental Table. The detailed information of the genes analyzed by real time RT-PCR

Gene	Official Gene symbol	Gene name	Assay ID
ACE2	*Ace2*	angiotensin I converting enzyme (peptidyl-dipeptidase A) 2	Mm01159003_m1
Mas	*Mas1*	MAS1 oncogene	Mm00434823_s1
BNP	*Nppb*	natriuretic peptide type B	Mm01255770_g1
αMHC	*Myh6*	myosin, heavy polypeptide 6, cardiac muscle, alpha	Mm00440346_g1
βMHC	*Myh7*	myosin, heavy polypeptide 7, cardiac muscle, beta	Mm00600532_g1
TGFβ1	*Tgfb1*	transforming growth factor, beta 1	Mm01178820_m1
collagen I	*Col1a1*	collagen, type I, alpha 1	Mm00801666_g1
Nox2	*Cybb*	cytochrome b-245, beta polypeptide	Mm01287743_m1
Nox4	*Nox4*	NADPH oxidase 4	Mm00479246_m1
GAPDH	*Gapdh*	glyceraldehyde-3-phosphate dehydrogenase	Mm99999915_g1

All primers and Taqman probes were purchased from Life Technologies. Assay ID indicates product number.